Fine Tuning of HOMO Energy Levels for Low-Band-Gap Photovoltaic Copolymers Containing Cyclopentadithienopyrrole and Bithiazole Units

Dhananjaya Patra, Duryodhan Sahu, Harihara Padhy, Dhananjay Kekuda, Chih-Wei Chu,* Kung-Hwa Wei, Hong-Cheu Lin*

Five conjugated LBG polymers P1–P5 consisting of a DTP unit as an electron donor and various bithiazole units as electron acceptors are designed and synthesized for photovoltaic applications. The effects of the electron-deficient bithiazole derivatives on the thermal, optical, electrochemical, and photovoltaic properties are investigated. The molecular structures are confirmed and characterized. The resulting polymers have high thermal stabilities and broad absorption bands with low optical bandgaps. The hole and electron mobilities are calculated. PSC devices are fabricated utilizing the polymers as electron donors and PCBM as an electron acceptor. The PSC device with an active layer of P4:PCBM (1:1 by weight) exhibits the best power-conversion efficiency.

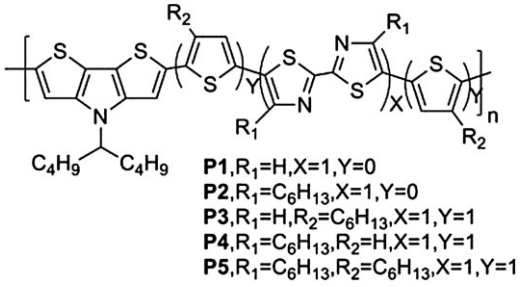

Introduction

Solar energy is one of the key alternatives to fossil fuels, due to the growing demands for clean, green, and sustainable energy. In the past decade, polymer solar cells have been an extensive area of research compared with the traditional, inorganic silicon counterpart, owing to their unique advantages, such as low cost and the ease of manufacturing thin films by vacuum deposition, solution casting, and printing technologies.[1] Moreover, these carbon-based materials can be engineered at the molecular level to have tunable electronic and optical properties. Syntheses of new conjugated polymers and small molecules has become an emerging area after the concept of bulk heterojunction (BHJ) polymer solar cells (PSCs) significantly improved power conversion efficiency (PCE) values over 7%[2] by the formation of a donor/acceptor (D-A), bicontinuous, interpenetrated network. Such a network creates large interfacial areas between the electron-donor polymers and the electron acceptors (such as fullerene derivatives) in the active-layer blend and leads to an efficient photoinduced charge transfer in PSC devices.

Efficient BHJ-PSC device architectures have been obtained using an active layer of poly(3-hexylthiophene) (P3HT) as an electron donor and [6,6]-phenyl-C_{61}-butyric acid methyl ester (PCBM) as an electron acceptor. Such systems have reached PCE values of up to 5%.[3] The main disadvantage of P3HT is its appreciably wide bandgap

D. Patra, H. Padhy, K.-H. Wei, H.-C. Lin
Department of Materials Science and Engineering, National Chiao Tung University, Hsinchu, Taiwan
E-mail: linhc@mail.nctu.edu.tw
D. Sahu, D. Kekuda, C.-W. Chu
Research Center for Applied Sciences, Academia Sinica, Taipei, Taiwan
E-mail: gchu@gate.sinica.edu.tw
C.-W. Chu
Department of Photonics, National Chiao Tung University, Hsinchu, Taiwan

DOI: 10.1002/macp.201100164

(1.9 eV); thus, it is only able to absorb 22% of the flux from the solar spectrum, as the maximum photon flux from the sun to the Earth's surface is approximately 1.8 eV (i.e., 700 nm). In order to solve this problem, several studies have been published in last 5 years on low-bandgap (LBG) D-A conjugated polymers: such materials offer unique advantages such as broad absorption bands, the tuning of the molecular energy levels [highest occupied molecular orbital (HOMO), and lowest unoccupied molecular orbital (LUMO)] and high charge-carrier mobilities.[4–5] In BHJ solar cells where PCBM is used as an acceptor, the ideal bandgap (in order to achieve a high V_{oc} value) of the donor polymer should be in the range of 1.2–1.9 eV, which corresponds to a HOMO energy level between −5.8 and −5.2 eV and a LUMO energy level between −4.0 and −3.8 eV.[1c–d] In such conjugated polymers, electron-donating groups and electron-withdrawing groups are substituted alternatively in the polymer backbones to lower the HOMO energy levels,[6] because the V_{oc} value is directly proportional to the difference between the HOMO level of the polymer and the LUMO level of the PCBM derivatives.[7] However, a large power–conversion-efficiency (PCE) value does not only rely upon a high V_{oc} value, but also requires an improved current density (J_{sc}) and fill factor (FF). LBG polymers possessing high charge-carrier mobilities are required for tuning high light-harvesting capabilities and lead to high J_{sc} and PCE values for PSC devices.[6] Moreover, high molecular weights, excellent solubilities and optimal morphologies are necessary to enhance the J_{sc} and FF values.[4a] Therefore, the molecular design of D-A alternating architectures in polymer backbones has received considerable attention from organic chemists for the development and application of new, low-bandgap conjugated polymers in photovoltaic devices.

For competent LBG polymer design, various electron-rich and electron-deficient building blocks, such as fluorene,[8] carbazole,[9] cyclopentadithiophene,[10] dithienopyrrole,[11] benzodithiophene,[12] thiadiazole,[13] thienopyrazine,[14] and quinoxaline,[15] have been utilized for optoelectronic applications. Dithieno[3,2-b:2′,3′-d]pyrroles (DTPs) (i.e., a kind of electron-rich building block containing fused thiophene units) offer great processabilities by attaching various alkyl chains to N-substituents of the pyrrole rings without affecting their conjugation lengths.[16] However, due to the high values of the HOMO levels in DTP-based polymers, they show relatively low V_{oc} values (less then 0.6 V), and thus induce low PCE values.[11c,17] This problem is expected to be solved by using various electron-deficient units to manipulate the HOMO energy levels. The thiazole unit is one of the five-membered azaheterocycles with electron-deficient characteristics and contains an electron-withdrawing imine (−C=N) in place of the carbon atom at the 3-position of the thiophene. Moreover, thiazole-based polymers have shown high oxidative stabilities that minimize the HOMO energy levels and induce high V_{oc} values.[18] Our previous approach reached a much higher PCE value of 3.04% by utilizing a copolymer containing bithiazole and cyclopentadithiophene units.[19] However, Li et al.[18b] have newly reported a D-A copolymer containing DTP and bithiazole moieties that only possessed a maximum PCE value of 0.06%. Wang et al.[11a] reported that an enhanced PCE value for PSC devices was obtained by decreasing the alkyl chain length (from eight to five) of the N-substituents in the DTP rings of a D-A copolymer containing benzothiadiazole units. In addition, McCullough et al.[5a] reported that some DTP-and-bithiazole-based polymers possess field-effect mobilities as high as $0.14\ cm^2 \cdot V^{-1} \cdot s^{-1}$.

In this report, a series of alternative D-A conjugated DTP-based polymers containing an electron-rich DTP block (with a minimum-branched alkyl chain length) and an electron-deficient bithiazole block are synthesized via Suzuki coupling polymerization. The manipulation of the optical, electrochemical, and photovoltaic properties by copolymerization with electron-deficient bithiazole derivatives is discussed. The preliminary PSC performance of these polymers blended with PCBM shows the best PCE value up to 0.69%, with $J_{sc} = 4.0\ mA \cdot cm^{-2}$, $V_{oc} = 0.40$ V, and FF = 0.43 under AM 1.5 ($100\ mW \cdot cm^{-2}$).

Experimental Section

Materials

All of the chemicals and solvents were reagent grade and were purchased from Aldrich, ACROS, Fluka, TCI, TEDIA, and Lancaster Chemical Co. Tetrahydrofuran (THF), toluene, and diethyl ether were distilled over sodium/benzophenone. Absolute ethanol was obtained by refluxing with magnesium ethoxide and then distilling. Other reagents were used as received without further purification.

Measurements and Characterization

^{1}H- and ^{13}C NMR spectra were recorded using a Varian Unity 300 MHz spectrometer using $CDCl_3$ as the solvent and the chemical shifts are reported as δ values relative to a tetramethylsilane (TMS) internal standard. Elemental analyses were performed using a Heraeus CHN-OS RAPID elemental analyzer. Thermogravimetric analyses were conducted using a TA Instruments Q500 instrument at a heating rate of $10\ ^\circ C \cdot min^{-1}$ under nitrogen. Gel permeation chromatography (GPC) was conducted using a Waters 1515 separation module, using polystyrene as a standard and THF as the eluent. UV-vis absorption spectra were recorded in dilute chlorobenzene solutions (10^{-6} M) using an HP G1103A spectrophotometer. Thin films for UV-vis measurements were spin-coated on glass substrates from chlorobenzene solution with a concentration of $5\ mg \cdot mL^{-1}$. Cyclic voltammetry (CV) was performed at a scanning rate of $100\ mV \cdot s^{-1}$ at room temperature using a BAS 100 electrochemical analyzer with a standard three-electrode electrochemical cell in 0.1 M tetrabutylammonium hexafluorophosphate ($TBAPF_6$) solution (in acetonitrile). During the CV measurements,

the solutions were purged with nitrogen for 30 s. In each case, a carbon rod coated with a thin layer of polymers as the working electrode, a platinum wire as the counter electrode, and a silver wire as the quasi-reference electrode were used. An Ag/AgCl (3 M KCl) electrode served as the reference electrode for all of the potentials quoted herein. The ferrocene/ferrocenium ion (Fc/Fc^+) redox couple was used as an external standard. The HOMO and LUMO energy levels were estimated by the onset oxidation and reduction potentials from the reference energy level of ferrocene (4.8 eV below the vacuum level), according to[19]

$$E_{\mathrm{HOMO/LUMO}} = \left[-\left(E_{\mathrm{onset}} - E_{\mathrm{onset}\left(\mathrm{FC/FC^+ vs. Ag/Ag^+}\right)}\right) - 4.8\right] \mathrm{eV} \quad (1)$$

$$\text{band gap} = E_{\mathrm{onset,ox}} - E_{\mathrm{onset,red}} \quad (2)$$

4.8 eV is the energy level of ferrocene below the vacuum level and $E_{\mathrm{onset}\left(\mathrm{FC/FC^+ vs. Ag/Ag^+}\right)} = 0.45$ eV. For the CV experiments with solid films of the polymers, which were performed by drop-casting films with similar thicknesses from THF solutions ($\approx 5\ \mathrm{mg \cdot mL^{-1}}$), the LUMO level of PCBM employed was in accordance with the literature data. The onset potentials were determined from the intersections of two tangents drawn at the rising currents and background currents of the CV measurements. Surface-morphology images of the thin films (on glass substrates) were obtained using atomic force microscopy (AFM, Digital Instruments NS 3a controller with a D3100 stage).

Fabrication of Polymer Solar Cells

The polymer photovoltaic (PV) cells in this study contained an active layer of copolymer (P1–P5) blended with PCBM in a solid film, which was sandwiched between a transparent indium/tin oxide (ITO) anode and a metal cathode (Ca). Prior to device fabrication, the ITO-coated glass substrates ($1.5 \times 1.5\ \mathrm{cm^2}$) were ultrasonically cleaned in detergent, deionized water, acetone, and isopropyl alcohol. After routine solvent cleaning, the substrates were treated with UV ozone for 15 min. Then, a modified ITO surface was obtained by the spin-coating of a layer of poly(ethylenedioxythiophene):poly(styrene sulfonate) (PEDOT:PSS) ($\approx$30 nm). After baking at 130 °C for 1 h, the substrates were transferred to a nitrogen-filled glove box. Subsequently, on the top of PEDOT:PSS layer, the active layer was prepared by spin-coating from blended solutions of polymers P1–P5:PCBM (with 1:1 w/w) at a spin rate of $\approx$1500 rpm. The thickness of the active layer was typically $\approx$80 nm. Initially, the blended solutions were prepared by dissolving both the polymer and PCBM in 1,2-dichlorobenzene (DCB) (20 mg:1 mL), followed by continuous stirring for 12 h at 50 °C. In the slow-growth approach, the blended polymers in solid films were kept in the liquid phase after spin-coating by using a solvent with a high boiling point (e.g., in a glass Petri dish) and allowing the solvent to dry slowly. Finally, a calcium layer (30 nm) and a subsequent aluminum layer (100 nm) were thermally evaporated through a shadow mask at a pressure below 6×10^{-6} Torr, to obtain an active device area of 0.12 $\mathrm{cm^2}$. The solar-cell testing was done inside a glove box under simulated AM 1.5G irradiation ($100\ \mathrm{mW \cdot cm^{-2}}$) using a xenon-lamp-based solar simulator (Thermal Oriel 1000 W). The light intensity was calibrated using a monosilicon photodiode with a KG-5 color filter (Hamamatsu). The external-quantum-efficiency (EQE) action spectra were obtained at short-circuit conditions. The light source was a 450 W Xe lamp (Oriel Instrument, model 6266) equipped with a water-based IR filter (Oriel Instruments, model 6123NS). The light output from the monochromator (Oriel Instruments, model 74100) was focused on the photovoltaic cell under test.

Fabrication of Hole- and Electron-Only Devices

The hole- and electron-only devices in this study contained polymer-blend films of P1–P5:PCBM (1:1 by weight) sandwiched between a transparent ITO anode and a cathode (MoO_3 and Ca, respectively). The devices were prepared following the same procedure as for the fabrication of BHJ devices, except that Ca was replaced with MoO_3 ($\Phi = 5.3$ eV) in the hole-only devices, and the PEDOT:PSS layer was replaced with Cs_2CO_3 ($\Phi = 2.9$ eV) in the electron-only devices. The MoO_3 was thermally evaporated to a thickness of 20 nm and capped with 50 nm of Al on the top of the active layer in the hole-only devices. Cs_2CO_3 was thermally evaporated with a thickness of approximately 2 nm on the transparent ITO in the electron-only devices. For both devices, annealing of the active layer was performed at 130 °C for 20 min.

Monomer Synthesis

4-(Nonan-5-yl)-4*H*-dithieno[3,2-b:2′,3′-d]pyrrole (1)

3,3′-Dibromo-2,2′-bithiophene (1 g, 3.08 mmol), t-BuONa (0.71 g, 7.40 mmol), tris(dibenzylideneacetone)dipalladium (Pd_2dba_3) (0.071 g, 0.007 mmol), and 2,2′-bis(diphenylphosphino)-1,1′-binaphthyl (BINAP) (0.288 g, 0.046 mmol) were dissolved in dry toluene (15 mL). The solution was purged with N_2 for 30 min. Nonan-5-amine (0.88 g, 6.17 mmol) was added via a syringe, and the mixture was stirred at 110 °C under N_2 for 12 h. After cooling, water was added to quench the reaction, and the solution was extracted twice with diethyl ether. The combined organic layer was dried over $MgSO_4$, and the solvent was removed by rotary evaporation. The crude product was purified by column chromatography on silica, using hexane as the eluent, to give a white solid (0.69 g, 73.3%).

^{1}H NMR (300 MHz, $CDCl_3$, δ): 7.10 (d, $J = 5.4$ Hz, 2H), 7.02 (d, $J = 5.4$ Hz, 2H), 4.26–4.16 (m, 1H), 1.96–1.82 (m, 2H), 1.81–1.32 (m, 2H), 1.14–1.05 (m, 8H), 0.88 (t, $J = 7.2$ Hz, 6H).

4-(Heptadecan-9-yl)-2,6-bis(4,4,5,5-tetramethyl-1,3,2-dioxaborolan-2-yl)-4*H*-dithieno[3,2-b:2′,3′-d]pyrrole (2)

Compound 1 (0.5 g, 1.63 mmol) was dissolved in 50 mL of dry THF, and the solution was cooled to −78 °C under nitrogen protection. Then, 0.65 mL of butyllithium (2.5 M in hexane, 3.26 mmol) was added, and the solution was warmed to room temperature for 30 min and cooled again to −78 °C. 2-Isopropoxy-4,4,5,5-tetramethyl-1,3,2-dioxaborolane (1.0 mL, 4.90 mmol) was rapidly injected into the solution using a syringe, and the resulting mixture was stirred at −78 °C for 1 h and left to stir overnight at room temperature. The resulting mixture was quenched with H_2O and extracted with dichloromethane (DCM). The DCM extracts were washed with saturated brine and dried with $MgSO_4$. The solvent was removed using a rotary evaporator and the product

was further purified by column chromatography on silica using a mixture of hexane and DCM (4:1) as the eluent to yield a white solid (0.49 g, 53.8%).

^{1}H NMR (300 MHz, $CDCl_3$, δ): 7.50 (s, 2H), 4.20 (m, 1H), 2.05–1.97 (m, 2H), 1.86–1.78 (m, 2H), 1.37 (s, 24H), 0.84 (t, $J = 6.0$ Hz, 6H); ^{13}C NMR (75 MHz, $CDCl_3$, δ): 147.78, 121.51, 120.68, 84.31, 60.26, 34.93, 29.07, 25.02, 22.60, 14.13; EIMS [M^+] calcd. $m/z = 557.42$; found 557.0. Anal. calcd. for $C_{29}H_{45}B_2NO_4S_2$: C 62.49, H 8.14, N 2.51; found: C 62.22, H 8.01, N 2.54.

4,4′-Dihexyl-5,5′-bis(4-hexylthiophen-2-yl)-2,2′-bithiazole (3)

2-(4-Hexylthiophen-2-yl)-4,4,5,5-tetramethyl-1,3,2-dioxaborolane (1.78 g, 6.06 mmol), tetrakis(triphenylphosphine)palladium [Pd(PPh3)4] (35 mg) and 10 mL of 2 M aqueous K_2CO_3 solution were added to a solution of monomer M2 (1 g, 2.02 mmol) in THF (30 mL). The reaction mixture was purged with N_2 and refluxed for 24 h. The reaction mixture was cooled to room temperature and extracted with DCM followed by washing with water and brine, and dried using anhydrous $MgSO_4$. The organic fraction was concentrated by rotary evaporation and the pure product was obtained by recrystallization from methanol as a yellow solid (1.09 g, 80.7%). ^{1}H NMR (300 MHz, $CDCl_3$, δ): 7.02 (s, 2H), 6.95 (s, 2H), 2.92 (t, $J = 6.0$ Hz, 4H), 2.61 (t, $J = 6.0$ Hz, 4H), 1.36–1.25 (m, 32H), 0.88 (t, $J = 6.0$ Hz, 12H).

5,5′-Bis(5-bromo-4-hexylthiophen-2-yl)-4,4′-dihexyl-2,2′-bithiazole (M5)

At room temperature, *N*-bromosuccinimide (NBS, 0.80 g, 4.48 mmol) was added portionwise to a solution of compound 3 (1.0 g, 1.49 mmol) in 25 mL of THF. After 30 min, water was added and the crude compound was extracted with DCM. The organic layer was washed with water and brine, and dried using anhydrous $MgSO_4$. The organic fraction was concentrated by rotary evaporation and the pure product was obtained by recrystallization from methanol as an orange solid (0.98 g, 79.7%).

^{1}H NMR (300 MHz, $CDCl_3$, δ): 6.87 (s, 2H), 2.87 (t, J = 6.0 Hz, 4H), 2.57 (t, J = 6.0 Hz, 4H), 1.36–1.25 (m, 32H), 0.89 (t, J = 6.0 Hz, 12H). ^{13}C NMR (75 MHz, $CDCl_3$, δ): 157.97, 154.98, 143.09, 132.62, 128.52, 122.52, 110.23, 31.82, 30.56, 29.80, 29.35, 22.80, 14.30. EIMS [M^+] calcd. $m/z = 658.60$; found 659.0. Anal. calcd. for $C_{38}H_{54}Br_2N_2S_4$: C 55.19, H 6.58, N 3.39; found: C 55.12, H 6.50, N 3.30.

General Polymerization Procedure

The synthetic routes to the polymers are shown in Scheme 1. All of the polymerization steps were carried out through palladium(0)-catalyzed Suzuki coupling reactions. In a 25 mL, flame-dried, two-necked flask, compound 2, the dibromo monomers (M1–M5), and $Pd(PPh_3)_4$ (0.5 mol%) were dissolved in a mixture of toluene (10 mL) and aqueous 2 M K_2CO_3 (5 mL). The reaction mixture was vigorously stirred at 90 °C for 3–4 d. After reaction, an excess of iodobenzene was added to the reaction; then, one hour later, an excess of phenylboronic acid was added and the reaction was refluxed overnight to complete the end-capping reaction. The polymer was purified by precipitation in methanol/water (10:1), filtered and washed with hexane, acetone, and chloroform using a Soxhlet apparatus. The chloroform fraction was reduced to 40–50 mL under reduced pressure, precipitated in methanol/water (10:1, 500 mL), filtered through 0.45 μm nylon filters, and finally air-dried overnight.

Polymer 1

Compound 2 (0.5 equiv.) and M1 (0.5 equiv.) were used in this polymerization following the general polymerization procedure, and the polymer was obtained as a black powder. Yield: 50%.

^{1}H NMR (300 MHz, $CDCl_3$, δ): 7.95 (s, 2H), 7.12 (s, 2H), 4.21 (m, 1H), 2.81 (br, 2H), 1.79–1.33 (br, 2H),1.15–1.03 (br, 8H), 0.86 (m, 6H); Anal. calcd for $C_{23}H_{25}N_3S_4$: C 58.56, H 5.34, N 8.91, S 27.19; found: C 58.06, H 5.13, N 8.22.

Polymer 2

Compound 2 (0.5 equiv.) and M2 (0.5 equiv.) were used in this polymerization following the general polymerization procedure, and the polymer was obtained as a black powder. Yield: 66%.

^{1}H NMR (300 MHz, $CDCl_3$, δ): 7.20 (s, 2H), 4.21 (m, 1H), 3.03 (m, 4H), 2.95–1.74 (br, m, 6H), 1.60–1.15 (br, m, 22H), 0.90–0.83 (m, 12H); Anal. calcd for $C_{35}H_{49}N_3S_4$: C 65.68, H 7.72, N 6.57, S 20.04; found: C 65.23, H 7.52, N 6.14.

Polymer 3

Compound 2 (0.5 equiv.) and M3 (0.5 equiv.) were used in this polymerization following the general polymerization procedure, and the polymer was obtained as a black powder. Yield: 62%.

^{1}H NMR (300 MHz, $CDCl_3$, δ): 7.95 (s, 2H), 7.20 (s, 4H), 4.21 (m, 1H), 2.93 (m, 4H), 2.95–1.70 (br, m, 6H), 1.61–1.11 (br, m, 22H), 0.90–0.83 (m, 12H); Anal. calcd for $C_{43}H_{53}N_3S_6$: C 64.21, H 6.64, N 5.22, S 23.92; found: C 63.71, H 6.64, N 5.05.

Polymer 4

Compound 2 (0.5 equiv.) and M4 (0.5 equiv.) were used in this polymerization following the general polymerization procedure, and the polymer was obtained as a black powder. Yield: 59%.

^{1}H NMR (300 MHz, $CDCl_3$, δ): 7.30–7.13 (s, 6H), 4.23 (m, 1H), 3.03 (m, 4H), 2.95–1.74 (br, m, 6H),1.61–1.13 (br, m, 22H), 0.90–0.83 (m, 12H); Anal. calcd for $C_{43}H_{53}N_3S_6$: C 64.21, H 6.64, N 5.22, S 23.92; found: C 65.11, H 6.34, N 5.41.

Polymer 5

Compound 2 (0.5 equiv.) and M5 (0.5 equiv.) were used in this polymerization following the general polymerization procedure, and the polymer was obtained as a dark-red powder. Yield: 61%.

^{1}H NMR (300 MHz, $CDCl_3$, δ): 7.20–6.91 (br, 4H), 4.21 (m, 1H), 3.03 (m, 10H), 2.95–1.74 (br, m, 10H),1.81–1.15 (br, m, 32H), 0.90–0.83 (m, 18H); Anal. calcd for $C_{55}H_{77}N_3S_6$: C 67.92, H 7.98, N 4.32, S 19.78; found: C 67.22, H 7.46, N 4.01.

Results and Discussion

Synthesis and Characterization

The synthetic routes for the monomer (M5) and the polymers are shown in Scheme 1. Synthesis of monomers M2 and M4 were reported previously,[9c] and monomer

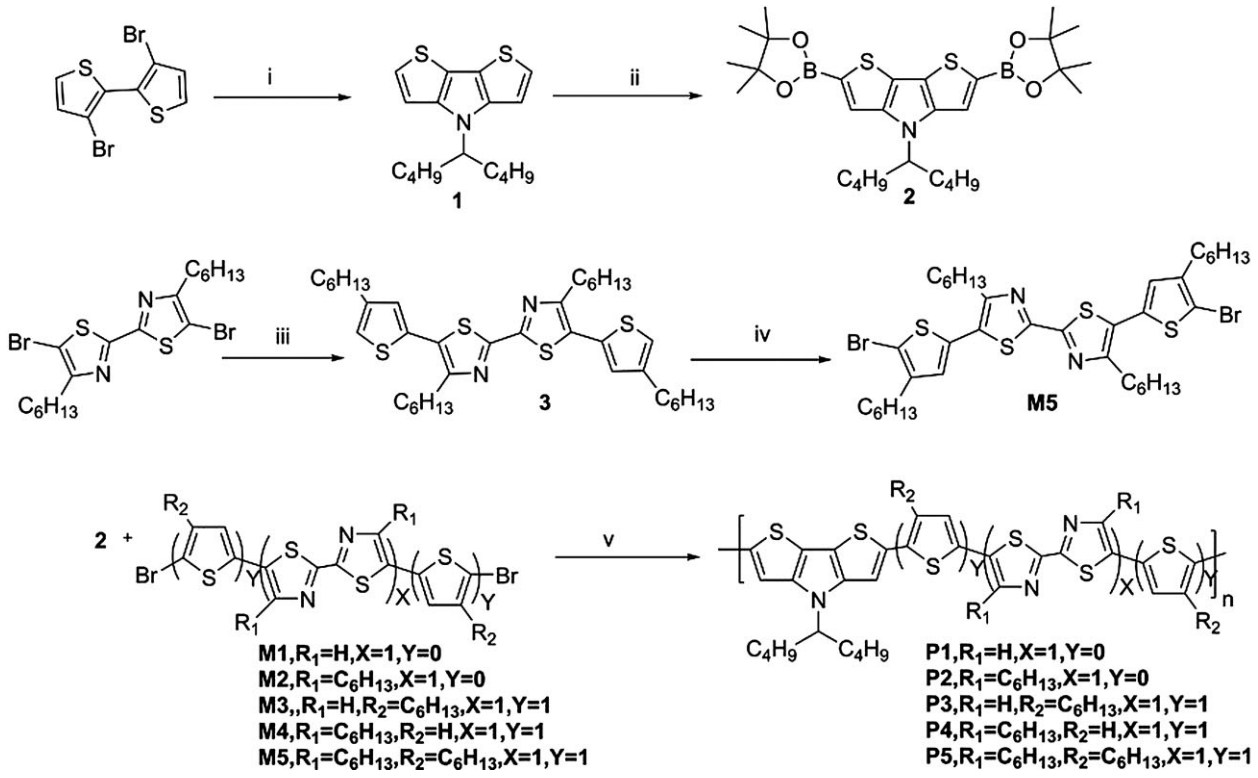

Scheme 1. Synthesis of M5 and polymers P1–P5. The reagents and conditions were: i) toluene, t-BuONa, Pd_2dba_3, BINAP, nonan-5-amine; ii) THF, butyllithium, 2-isopropoxy-4,4,5,5-tetramethyl-1,3,2-dioxaborolane, −78 °C; iii) THF, 2-(4-hexylthiophen-2-yl)-4,4,5,5-tetramethyl-1,3,2-dioxaborolane, $Pd(PPh_3)_4$, 24 h; iv) NBS, THF, 30 min; v) toluene, 2 M K_2CO_3, $Pd(PPh_3)_4$, 90 °C, 3–4 d.

M1[16c] and M3[20] were prepared by modified methods according to the literature. M2 was converted to compound 3 by a Suzuki coupling with 2-(4-hexylthiophen-2-yl)-4,4,5,5-tetramethyl-1,3,2-dioxaborolane[13a] and finally brominated with NBS to form M5. The donor moiety (1) [i.e., dithieno[3,2-b:2′,3′-d]pyrrole (DTP)] was synthesized via a Buchwald-Hartwig reaction of 3,3′-dibromo-2,2′-bithiophene[11a] and nonan-5-amine.[11b] Compound 1 was converted to compound 2 by deprotonation with butyllithium followed by addition of 2-isopropoxy-4,4,5,5-tetramethyl-1,3,2-dioxaborolane with a yield of 54%. Monomer M5, and compound 2 were satisfactorily characterized by ^{1}H NMR, ^{13}C NMR, and MS spectroscopy, and elemental analysis.

All of the polymers (P1–P5) were synthesized by Suzuki coupling polymerization in toluene between one electron-sufficient moiety (2) and five electron-deficient moieties (M1–M5). All of these polymers (except polymer P1) were readily soluble in organic solvents, such as chloroform, THF, and chlorobenzene at room temperature and completely soluble in high-boiling-point solvents (e.g., chlorobenzene) at high temperature. The average molecular weights ($\overline{M}_n$ and $\overline{M}_w$) of polymers P1–P5 determined by GPC against polystyrene standards in THF are summarized in Table 1. These results show that considerable molecular weights with moderate yields (50–66% after Soxhlet extractions) were obtained in these polymers, where the average molecular weights ($\overline{M}_w$) ranged from 11 200–91 000 with polydispersity indices (PDI $= \overline{M}_w/\overline{M}_n$) of 1.04–2.02.

The thermal stability of the conjugated polymer plays a key role for optoelectronic applications. The thermal stabilities of polymers P1–P5 were investigated using thermogravimetric analyses (TGA), and their corresponding results are summarized in Figure 1 and Table 1. It is apparent that all of the polymers exhibited good thermal stabilities as the temperatures for 5% weight loss (under nitrogen) were found to be 403–369 °C. These are adequate for applications in polymer solar cells and other optoelectronic devices.

Optical Properties

The photophysical characteristics of the polymers in chlorobenzene solution and as solid films were investigated by UV-vis absorption spectroscopy. The spectra are presented in Figure 2, and the absorption maxima (for both the solutions and the solid films) and the optical bandgaps ($E_{g,opt}$) are listed in Table 2. As expected, all of the electron donor/acceptor polymers demonstrated a red-shifted absorption from solution to the solid films. In

Table 1. Molecular weights and thermal properties of polymers P1–P5.

Polymer	$\overline{M}_w$ [a)] [g · mol^{-1}]	$\overline{M}_n$ [a)] [g · mol^{-1}]	PDI[a)]	Yield [%]	T_d [b)] [°C]
P1	11 133	10 681	1.04	50	389
P2	65 575	34 062	1.93	66	376
P3	91 059	44 987	2.02	62	370
P4	28 864	22 646	1.27	59	403
P5	12 560	10 884	1.15	61	369

[a)]The molecular weights ($\overline{M}_n$ and $\overline{M}_w$) and polydispersity indices were measured by GPC using THF as the eluent and polystyrene standards; [b)]Temperature of 5% weight loss measured by TGA at a heating rate of 10 °C · min^{-1} under nitrogen.

addition, the absorption maxima of polymers P1–P5 were in the range of 480–522 nm and 508–558 nm for solution and the solid films, respectively. As shown in Figure 2, similar intramolecular charge/transfer (ICT) interactions between the electron donor DTP and acceptor bithiazole derivatives were found in the UV-vis spectra of the rigid, π-conjugated, D-A polymers.[11b,c,19] Due to the presence of the various electron-donating moieties in polymers P2–P5, such as the alkyl chains (e.g., hexyl groups) on the thiophene and bithiazole units, different extents of red-shifted absorption occurred from the solutions to the solid films. Due to having the worst solubility in chlorobenzene solution, polymer P1 possessed the least red-shifted absorption maxima (3 nm) from solution to the solid film. Compared with polymers P3–P4, polymer P5 possesses blue-shifted absorption maxima in both solution and the solid film, which might be due to a twisting of the polymer backbones induced by the alkyl side-chains on both the bithiazole and thiophene units.[19] Compared with polymers P1 and P2 in the solid films, the corresponding P3 and P4 polymers possess 33 and 6 nm red-shifted absorption maxima, respectively, which implies that the electron-donating hexylthiophene units had a bigger contribution to broadening the conjugation

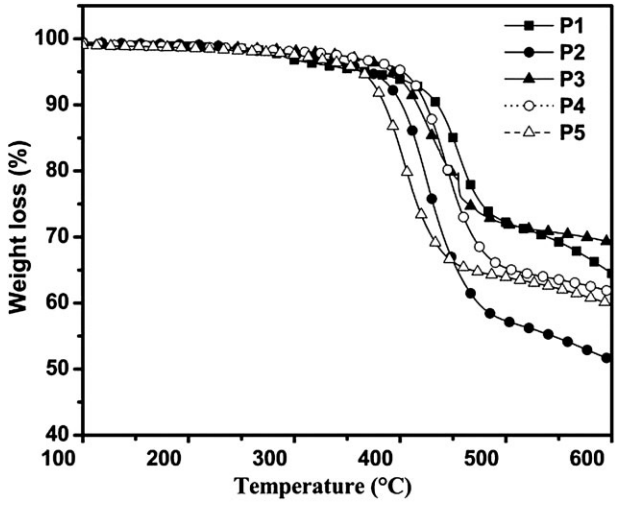

Figure 1. TGA measurements of polymers P1–P5 with a heating rate of 10 °C · min^{-1}.

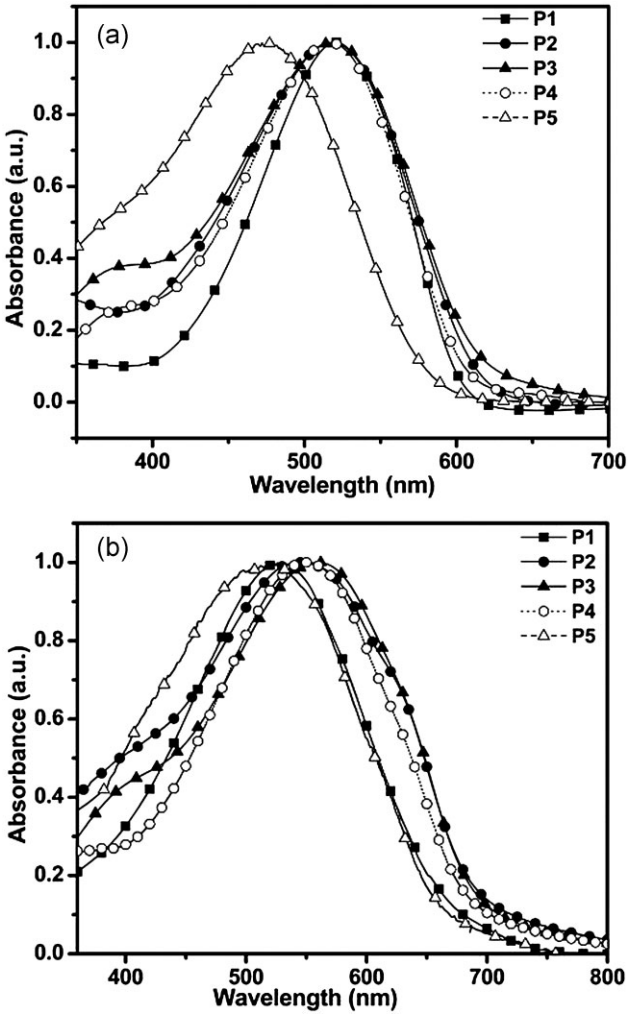

Figure 2. Normalized UV-vis spectra of polymers (a) in dilute chlorobenzene solution and (b) as solid films on glass surfaces.

Table 2. Optical and electrochemical data of polymers P1–P5.

Polymer	Solution[a)]	Solid film[b)]		Energy levels				Bandgap[d)]	
	$\lambda_{max,abs}$ [nm]	$\lambda_{max,abs}$ [nm]	$\lambda_{onset,abs}$ [nm]	$E_{onset,ox}$ [V]	E_{HOMO}[c)] [eV]	$E_{onset,red}$ [V]	E_{LUMO}[c)] [eV]	$E_{g,ec}$ [eV]	$E_{g,opt}$ [eV]
P1	522	525	704	0.93	−5.28	−0.62	−3.76	1.52	1.76
P2	518	543	712	0.82	−5.17	−0.81	−3.54	1.63	1.74
P3	519	558	725	0.63	−4.99	−0.77	−3.55	1.40	1.71
P4	517	549	734	0.49	−4.81	−0.84	−3.59	1.33	1.68
P5	480	508	691	0.71	−5.06	−0.64	−3.71	1.35	1.79

[a)] Chlorobenzene solution (10^{-6} M); [b)] Spin-coated from chlorobenzene solution on a glass surface; [c)] $E_{HOMO/LUMO} = \left[-\left(E_{onset} - E_{onset(FC/FC^+ vs.Ag/Ag^+)}\right) - 4.8\right]$ eV, where 4.8 eV is the energy level of ferrocene below the vacuum level and $E_{onset(FC/FC^+ vs.Ag/Ag^+)} = 0.45$ eV; [d)] Bandgaps: electrochemical bandgap $E_{g,ec} = E_{onset,ox} - E_{onset,red}$ and optical bandgap $E_{g,opt} = 1\,240/\lambda_{edge}$.

lengths in the copolymers than the thiophene units.[15] The optical bandgaps ($E_{g,opt}$) of the polymers in the solid films were determined by the cut-off wavelengths of the optical absorptions are in the range of 1.68–1.79 eV (see Table 2). Moreover, the optical bandgaps of the polymers could be lowered to the narrowest value of $E_{g,opt} = 1.68$ eV (or $E_{g,ec} = 1.33$ eV) for P4. These results imply that it is an efficient way to design the DTP-based photovoltaic polymers to have higher light-harvesting capabilities by tuning the various electron-donating moieties in the electron-deficient bithiazole derivatives.

Electrochemical Properties

To investigate the redox behavior of the random copolymers and their electronic states (i.e., the HOMO/LUMO levels), the electrochemical properties of polymers P1–P5 were investigated by CV. The oxidation and reduction cyclic voltammograms of the polymers are shown in Figure 3. The electrochemical properties, such as the onset potentials of oxidation and reduction, [i.e., the estimated positions of the upper edges of the valence bands (HOMO) and the lower edges of the conduction bands (LUMO), respectively] and the electrochemical bandgaps of all of the polymers are summarized in Table 2. It can be seen that polymers P1–P2 possessed one, and P3–P5 possessed two quasi-reversible or reversible p-doping/dedoping (oxidation/re-reduction) processes at positive potential ranges and one reversible n-doping/dedoping (reduction/reoxidation) process at negative potential ranges. All of these polymers exhibited oxidation (p-doping) due to the electron-rich DTP units and reduction (n-doping) because of the electron-deficient bithiazole derivatives.[16c]

The moderate onset oxidation and reduction potentials of polymers P1–P5 occurred between 0.49–0.93 and (−0.62)–(−0.84) V, respectively. The estimated HOMO and LUMO levels for polymers P1–P5 were found to be −4.81 to −5.28 eV and −3.54 to −3.76 eV, respectively, which is in good agreement with previously reported results. The electrochemical bandgaps calculated from the differences between the oxidation and reduction potentials were found to be in the range of 1.33–1.63 eV for polymers P1–P5. Polymers P1–P2 possessed relatively lower HOMO energy levels compared with polymers P3–P5 due to their high-onset oxidation potentials. By adding two alkyl chains to the bithiazole rings of P1, the rigidity and oxidation potential of P2 were reduced; thus, the HOMO energy level of P1 was lower than P2.[16c] The presence of electron-rich species (thiophene or hexylthiophene) maximized the HOMO energy levels of polymers P3–P5 compared with polymers P1–P2.[17] Hence, increasing the electron-donating moieties in the polymer backbones lowers the bandgap

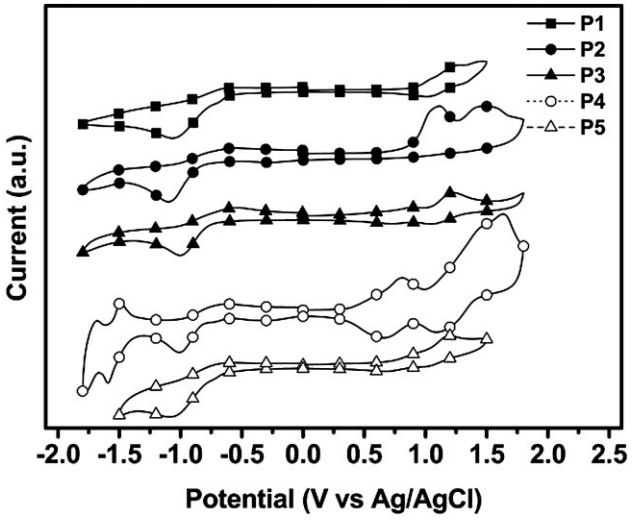

Figure 3. Cyclic voltammograms of P1–P5 in solid films at a scan rate of 100 mV · s^{-1}.

and oxidation potentials.[16a] DTP-based polymers possessing similar LUMO energy levels suggest that electron-deficient bithiazole derivatives have similar accepting capabilities.[16c] The electrochemical bandgaps of all of the polymers were smaller than the corresponding optical bandgaps, which might be due to interfacial energy barriers present between the polymer films and the electrode surfaces.[21] The LUMO energy levels of the donor polymers should be positioned above the LUMO energy levels of the acceptor PCBM by at least 0.3 eV so that the exciton binding energies of the polymers can be overcome and can result in efficient electron transfer from the electron donors to the acceptors. The high reduction potentials of polymers P1–P5 represent high electron affinities, making these polymers suitable donors for injecting and transporting electrons to the acceptor PCBM for polymer solar-cell devices.

Photovoltaic Cell Properties

The motivation to design and synthesize these DTP-based copolymers is to look for new LBG polymers for the application of PSCs. BHJ photovoltaic devices were fabricated with a configuration of ITO/PEDOT:PSS (30 nm)/(P1–P5):PCBM (≈80 nm) (1:1 w/w)/Ca (30 nm)/Al (100 nm). Figure 4a presents the current/voltage (*J*/*V*) curves for the copolymers under the condition of AM 1.5 at 100 mW · cm^{-2}; the photovoltaic properties, including the open-circuit voltage (V_{oc}), short-circuit current density (J_{sc}), fill factor (FF), and PCE values of the PSC devices are summarized in Table 3.

The solar-cell devices based on polymers P1–P5 showed different V_{oc} values in the range of 0.18–0.62 V, which are related to the differences between the HOMO energy levels of the polymers and the LUMO energy levels of the acceptors. However, a low V_{oc} (0.28 V) value obtained from the DTP-and-bithiazole-based polymer reported by Li. et al.[18b] reflected a low PCE. The oxidation potential of polymer P1 incorporated with the electron-withdrawing bithiazole unit showed a higher value, so polymer P1 showed the deepest HOMO level among all of the polymers. It is clear that electron-deficient bithiazole unit has a strong tendency to enhance the oxidation strength (high oxidation state) of the polymer. On the other hand, the addition of electron-donating moieties to bithiazole derivatives causes the reduction of oxidation potentials in polymers P1–P5 and increases their HOMO values. Unfortunately, polymer P1 showed the lowest PCE value of 0.06%, which is attributed to its poor solubility and film-forming quality. Polymer P2 achieved a much-higher V_{oc} value in the DTP-and-bithiazole-based polymers, owing to its lower HOMO level.[18b] The V_{oc} values gradually decreased among polymers P2–P4 due to the enhancement of the HOMO values in the polymers.

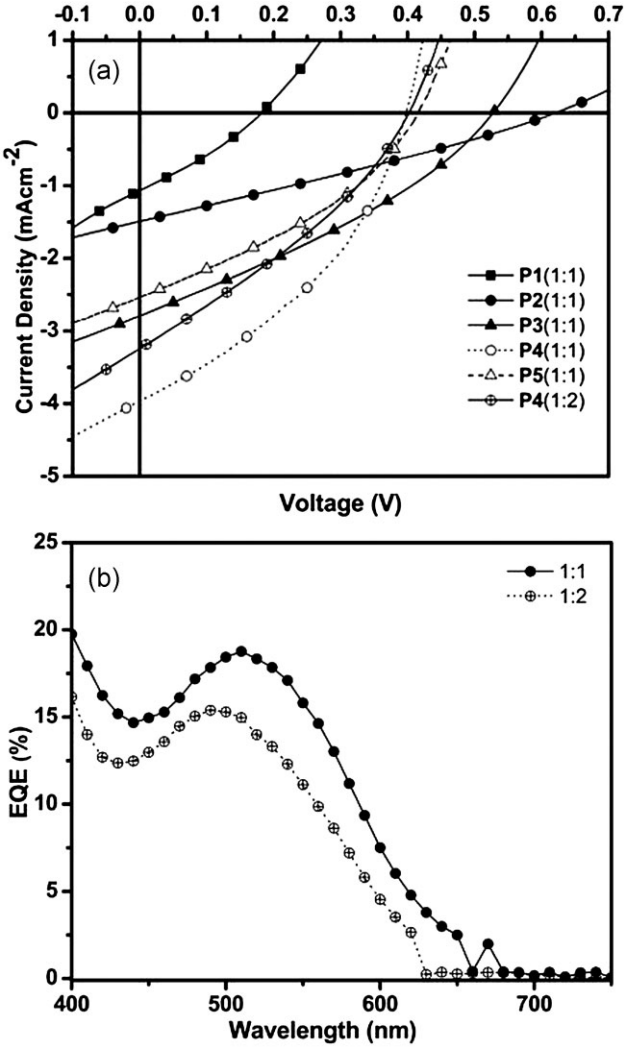

Figure 4. a) *J*/*V* characteristics of ITO/PEDOT:PSS/P1–P5:PCBM (1:1 or 1:2 by weight)/Ca/Al under illumination of AM 1.5 at 100 mW · cm^{-2}. b) EQE curves for PSC devices based on the P4:PCBM polymer blends at two weight ratios (1:1 and 1:2).

The charge-transport properties, including the hole and electron mobilities, are the key parameters for both material design and device fabrication.[4] The hole and electron mobilities were determined precisely by fitting the plot of dark current versus voltage (*J*/*V*) for single-carrier devices to the space-charge limit current (SCLC) model. The dark current is given by

$$J = \frac{9\varepsilon_0\varepsilon_r\mu V^2}{8L^3} \quad (3)$$

where ε_0 ε_r is the permittivity of the polymer, μ is the carrier mobility and L is the device thickness. As shown in Table 3, the hole and electron mobilities of polymers P1–P5 were found to be in the ranges of 10^{-8}–10^{-7} and 10^{-7}–

Table 3. Electron and hole mobilities, photovoltaic properties, and roughness (R_{rms}) of polymers P1–P5.

Polymer blend (P:PCBM weight ratio)	Electron mobility μ_e [$cm^2 \cdot V^{-1} \cdot s^{-1}$]	Hole mobility μ_h [$cm^2 \cdot V^{-1} \cdot s^{-1}$]	μ_e/μ_h	J_{sc} [$mA \cdot cm^{-2}$]	V_{oc} [V]	FF	PCE [%]	R_{rms} [nm]
P1 (1:1)	2.97×10^{-6}	9.64×10^{-8}	30.8	1.1	0.18	0.34	0.06	0.39
P2 (1:1)	1.23×10^{-6}	3.22×10^{-8}	23.5	1.5	0.62	0.29	0.27	0.36
P3 (1:1)	9.63×10^{-7}	5.30×10^{-8}	18.2	2.8	0.53	0.32	0.47	0.25
P4 (1:1)	1.21×10^{-6}	2.17×10^{-7}	5.6	4.0	0.40	0.43	0.69	0.22
P5 (1:1)	8.29×10^{-6}	4.16×10^{-8}	19.9	2.5	0.41	0.35	0.36	0.25
P4 (1:2)	–	–	–	3.2	0.40	0.43	0.55	0.32

10^{-6} $cm^2 \cdot V^{-1} \cdot s^{-1}$, respectively. The electron mobilities are much higher (i.e., approximately one order of magnitude) than the hole mobilities, resulting in an imbalance in the transport of holes and electrons in the polymer-active layer. The highest hole mobility was found to be 2.17×10^{-7} $cm^2 \cdot V^{-1} \cdot s^{-1}$ for polymer P4, which is the key parameter for the highest J_{sc} value among all of the polymers. Furthermore, the balance ratio of 5.6 for the two charge-transport mechanisms ($\mu_e/\mu_h = 5.6$) was found to be the lowest for polymer P4, which is also another reason to explain the highest PCE value for P4 for all of the polymers P1–P5.[13b] All of the polymers showed poor mobilities, which may be attributed to the molecular weight[22] and the low FF values: this could be due to the imbalance of the hole and electron transport in the polymer active layer.[13C] By increasing the weight ratios of the polymer P4:PCBM from 1:1 to 1:2, lower J_{sc} and PCE values were observed. In order to further explain the lower efficiency (0.55%) of P4, the EQE spectra of the PSC devices containing polymer P4 with various ratios of PCBM (1:1 and 1:2 by weight) are presented in Figure 4b. The maximum EQE values of the PSC devices containing P4 in the ratios of 1:1 and 1:2 were found to be 20% and 15%, respectively (at 500–520 nm).

The surface morphology of the active layer in the PSC devices is also a key parameter for the device performance.[13b,c] AFM topographic images of polymer blends P1-P5:PCBM (1:1 by weight) and P4:PCBM (1:2 by weight) are presented in Figure 5 and their root-mean-square values of roughness (R_{rms}) are shown in Table 3. It is clear that the phase images of all of the surfaces possess almost-similar roughness, which was attributed to domains of the highly stacked polymer chains.[19] The roughest and least-rough surfaces were found to be $R_{rms} = 0.39$ and 0.22 nm in polymer blends P1 and P4 (with PCBM = 1:1 by weight), respectively, where polymer blend P1:PCBM (1:1 w/w) possessed a larger-scale phase separation and thus induced the lowest PCE value (0.06%). This low PCE value of the P1:PCBM (1:1 w/w) polymer blend might originate from the reduced diffusional-escape probability for mobile charge carriers and consequently to the increase in charge recombination.[8b,9c] As a result, polymer blends P1 and P4 possessed the least and highest J_{sc} values, correspondingly. However, polymer P4 blended with the higher weight ratio of PCBM (P4:PCBM = 1:2 by weight) possessed a lower J_{sc} value, due to a larger phase separation, indicated by the larger roughness ($R_{rms} = 0.32$ nm). However, Li et al.[18b] reported that one D-A copolymer containing DTP and bithiazole moieties as electron-donor and electron-acceptor segments, respectively, possessed a maximum PCE value of 0.06%, with $V_{oc} = 0.28$ V, $J_{sc} = 0.51$ $mA \cdot cm^{-2}$, and FF = 0.34. The most efficient PSC device in this report with the maximum PCE value of 0.69% was established by the polymer blend of P4 and PCBM (with a weight ratio of 1:1).

Conclusion

Five DTP-based low-bandgap photovoltaic polymers (P1–P5) containing an electron-donor dithienopyrrole (DTP) unit and various electron-acceptor bithiazole derivatives were designed and synthesized via a palladium-catalyzed Suzuki coupling polymerization. The optical properties revealed that these new copolymers exhibit strong π-π stacking and an enhanced absorption-maximum band in solid films due to strong ICT in the polymer backbone. The HOMO and LUMO energy levels of the DTP-based polymers can be finely tuned to the ranges of −5.28 to −4.81 and −3.76 to −3.54 eV by copolymerization with electron-deficient bithiazole derivatives. Among the photovoltaic devices fabricated from the active layer of polymer blends of P1–P5:PCBM in a weight ratio of 1:1, the one containing P4 offered the best performance of PCE = 0.69%, with $V_{oc} = 0.40$ V, $J_{sc} = 4.0$ $mA \cdot cm^{-2}$, and FF = 0.43 under AM 1.5 global-illumination conditions. Therefore, tunable optical, electrochemical, and photovoltaic properties could be obtained by attaching lateral segments (such as hexyl chains) and conjugated

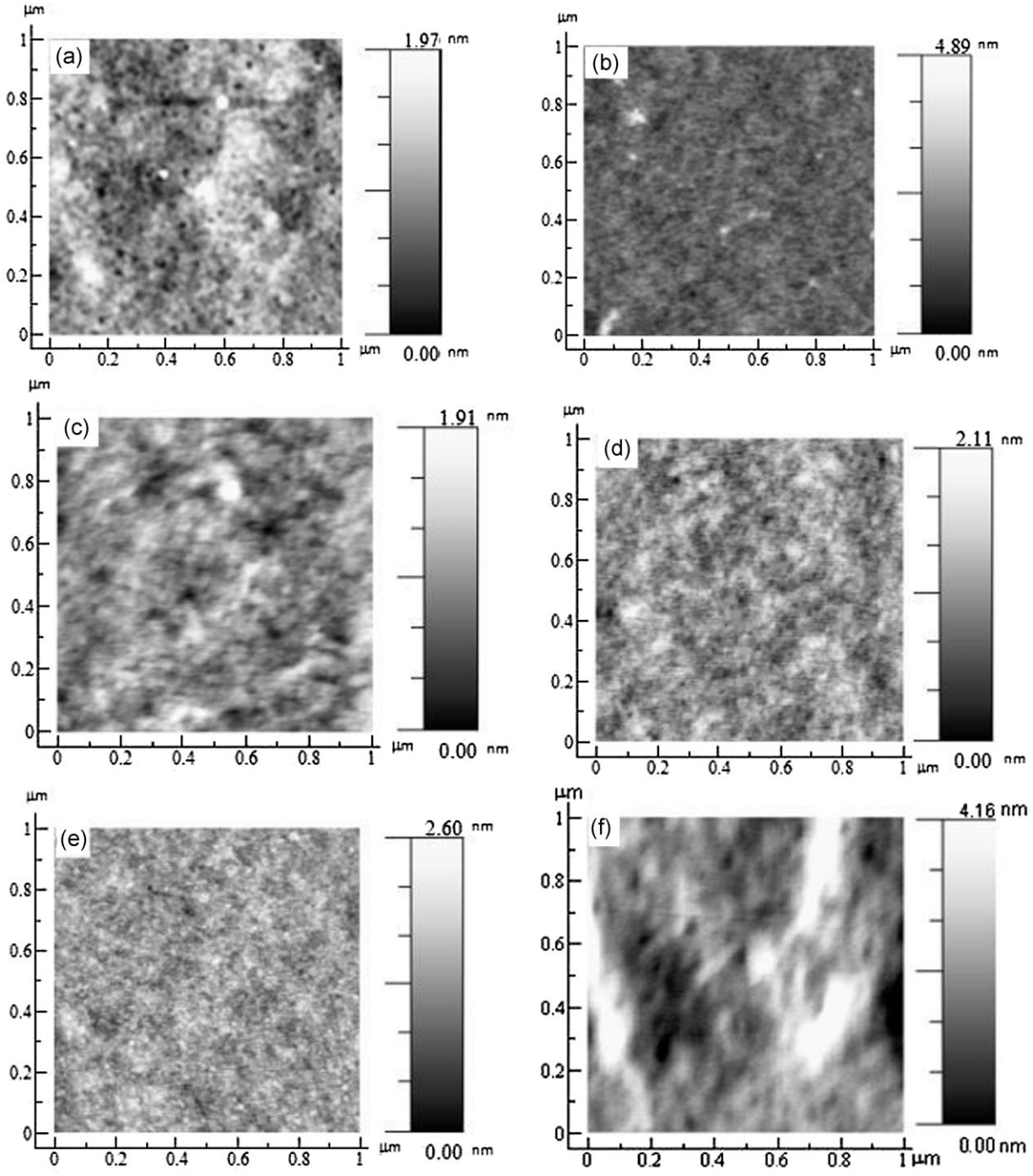

Figure 5. AFM images of polymers: (a) P1, (b) P2, (c) P3, (d) P4, and (e) P5, each blended with PCBM in the P1–P5:PCBM weight ratio of 1:1 (w/w). f) AFM image of P4:PCBM in the weight ratio of 1:2 (w/w). The polymers were spin-coated from DCB, with a size of $1 \times 1\,\mu m^2$.

linkers (such as thiophene and hexylthiophene units) to the bithiazole moieties in the polymer backbones.

Acknowledgements: We are grateful to the National Center for High-Performance Computing for computer time and facilities. Financial support of this project provided by the National Science Council of Taiwan (China) through NSC 97-2113-M-009-006-MY2, the National Chiao Tung University through 97W807, and the Energy and Environmental Laboratories (led by Dr. Chang-Chung Yang) at the Industrial Technology Research Institute (ITRI) is acknowledged.

Received: March 21, 2011; Revised: May 17, 2011; Published online: July 28, 2011; DOI: 10.1002/macp.201100164

Keywords: bithiazoles; conjugated polymers; dithienopyrroles; low bandgaps; synthesis

[1] [1a] Y. J. Cheng, S. H. Yang, C. S. Hsu, *Chem. Rev.* **2009**, *109*, 5868; [1b] E. Bundgaard, F. C. Krebs, *Sol. Energy Mater Sol. Cells* **2007**, *91*, 954; [1c] B. C. Thompson, J. M. J. Frechet, *Angew. Chem. Int. Ed.* **2008**, *47*, 58; [1d] S. Günes, H. Neugebauer, N. S. Sariciftci, *Chem. Rev.* **2007**, *107*, 1324.

[2] [2a] T.-Y. Chu, J. Lu, S. Beaupré, Y. Zhang, J.-R. Pouliot, S. Wakim, J. Zhou, M. Leclerc, Z. Li, J. Ding, Y. Tao, *J. Am. Chem. Soc.* **2011**, *133*, 4250; [2b] S. C. Price, A. C. Stuart, L. Yang, H. Zhou, W. You, *J. Am. Chem. Soc.* **2011**, *133*, 4625; [2c] H. Zhou, L. Yang, A. C. Stuart, S. C. Price, S. Liu, W. You, *Angew. Chem. Int. Ed.* **2011**, *50*, 2995.

[3] [3a] G. Li, V. Shrotriya, J. S. Huang, Y. Yao, T. Moriarty, K. Emery, Y. Yang, *Nat. Mater.* **2005**, *4*, 86; [3b] W. L. Ma, C. Y. Yang, X. Gong, K. H. Lee, A. J. Heeger, *Adv. Funct. Mater.* **2005**, *15*, 1617.

[4] [4a] S. C. Price, A. C. Stuart, Y. You, *Macromolecules* **2010**, *43*, 4609; [4b] P. Ding, C.-C. Chu, B. Liu, B. Peng, Y. Zou, Y. He, K. Zhou, C.-S. Hsu, *Macromol. Chem. Phys.* **2010**, *211*, 2555.

[5] [5a] J. Liu, R. Zhang, I. Osaka, S. Mishra, A. E. Javier, D.-M. Smilgies, T. Kowalewski, R. D. McCullough, *Adv. Funct. Mater.* **2009**, *19*, 3427; [5b] M. Yang, B. Peng, B. Liu, Y. Zou, K. Zhou, Y. He, C. Pan, Y. Li, *J. Phys. Chem. C* **2010**, *114*, 17989.

[6] [6a] H. Zhou, L. Yang, S. Stoneking, W. You, *ACS Appl. Mater. Interfaces* **2010**, *2*, 1377; [6b] M. Zhang, H. Fan, X. Guo, Y. He, Z.-G. Zhang, J. Min, J. Zhang, G. Zhao, X. Zhan, Y. Li, *Macromolecules* **2010**, *43*, 8714.

[7] C. J. Brabec, N. S. Sariciftci, J. C. Hummelen, *Adv. Funct. Mater.* **2001**, *11*, 15.

[8] [8a] K. C. Li, Y. C. Hsu, J. T. Lin, C. C. Yang, K. W. Wei, H. C. Lin, *J. Polym. Sci., Part A: Polym. Chem.* **2008**, *46*, 4285; [8b] Y. Li, Z. Li, C. Wang, H. Li, H. Lu, B. Xu, W. Tian, *J. Polym. Sci., Part A: Polym. Chem.* **2008**, *46*, 2765.

[9] [9a] N. Blouin, A. Michaud, D. Gendron, S. Wakim, E. Blair, R. Neaguplesu, M. Belletete, G. Durocher, Y. Tao, M. Leclerc, *J. Am. Chem. Soc.* **2008**, *130*, 732; [9b] B. Peng, B. Liu, A. Najari, P. Berrouard, D. Gendron, Y. He, K. Zhou, Y. Zou, M. Leclerc, *Macromol. Chem. Phys.* **2010**, *211*, 2026; [9c] D. Patra, D. Sahu, H. Padhy, D. Kekuda, C.-W. Chu, H.-C. Lin, *J. Polym. Sci., Part A: Polym. Chem.* **2010**, *48*, 5479.

[10] [10a] J. Peet, J. Y. Kim, N. E. Coates, W. L. Ma, D. Moses, A. J. Heeger, G. C. Bazan, *Nat. Mater.* **2007**, *6*, 497; [10b] G.-Y. Chen, C.-M. Chiang, D. Kekuda, S.-C. Lan, C.-W. Chu, K.-H. Wei, *J. Polym. Sci. Part A: Polym. Chem.* **2010**, *48*, 1669; [10c] M.-C. Yuan, M.-Y. Chiu, C.-M. Chiang, K.-H. Wei, *Macromolecules* **2010**, *43*, 6270.

[11] [11a] W. Yue, Y. Zhao, S. Shao, H. Tian, Z. Xie, Y. Geng, F. Wang, *J. Mater. Chem.* **2009**, *19*, 2199; [11b] D. Sahu, H. Padhy, D. Patra, J.-H. Huang, C.-W. Chu, H.-C. Lin, *J. Polym. Sci., Part A: Polym. Chem.* **2010**, *48*, 5812; [11c] E. Zhou, J. Cong, K. Tajima, C. Yang, K. Hashimoto, *Macromol. Chem. Phys.* **2011**, *212*, 305.

[12] [12a] P. Ding, C.-C. Chu, B. Liu, B. Peng, Y. Zou, Y. He, K. Zhou, C.-S. Hsu, *Macromol. Chem. Phys.* **2010**, *211*, 2555; [12b] G. Zhang, Y. Fu, Q. Zhang, Z. Xie, *Macromol. Chem. Phys.* **2010**, *211*, 2596.

[13] [13a] H. Padhy, J.-H. Huang, D. Sahu, D. Patra, D. Kekuda, C.-W. Chu, H.-C. Lin, *J. Polym. Sci., Part A: Polym. Chem.* **2010**, *48*, 4823; [13b] J. Hou, T. L. Chen, S. Zhang, H.-Y. Chen, Y. Yang, *J. Phys. Chem. C* **2009**, *113*, 1601; [13c] Y.-C. Chen, C.-Y. Yu, Y.-L. Fan, L.-I. Hung, C.-P. Chen, C. Ting, *Chem. Commun.* **2010**, 6503.

[14] [14a] R. Mondal, S. Ko, Z. Bao, *J. Mater. Chem.* **2010**, *20*, 10568; [14b] M.-H. Lai, J.-H. Tsai, C.-C. Chueh, C.-F. Wang, W.-C. Chen, *Macromol. Chem. Phys.* **2010**, *211*, 2017.

[15] [15a] M. H. Petersen, O. Hagemann, K. T. Nielsen, M. Jørgensen, F. C. Krebs, *Sol. Energy Mater. Sol. Cells* **2007**, *91*, 996; [15b] E. Zhou, J. Cong, K. Tajima, K. Hashimoto, *Chem. Mater.* **2010**, *22*, 4890.

[16] [16a] J. Roncali, *Chem. Rev.* **1997**, *97*, 173; [16b] S. Zhag, Y. Guo, H. Fan, Y. Liu, H.-Y. Chen, G. Yang, X. Zhan, Y. Liu, Y. Li, Y. Yang, *J. Polym. Sci., Part A: Polym. Chem.* **2009**, *47*, 5498; [16c] I. H. Jung, J. Yu, E. Jeong, S. Kwon, H. Kong, K. Lee, H. Y. Woo, H. K. Shim, *Chem. Eur. J.* **2010**, *16*, 3743.

[17] X. Zhang, T. T. Steckler, R. R. Dasari, S. Ohira, W. J. Potscavage, Jr, S. P. Tiwari, S. Coppée, S. Ellinge, S. Barlow, J.-L. Brédas, B. Kippelen, J. R. Reynolds, S. R. Marder, *J. Mater. Chem.* **2010**, *20*, 123.

[18] [18a] W.-Y. Wong, X.-Z. Wang, Z. He, K.-K. Chen, A. B. Djurišić, K.-Y. Cheung, C.-T. Yip, A. M.-C. Ng, Y. Y. Xi, C. S. K. Mak, W.-K. Chan, *J. Am. Chem. Soc.* **2007**, *129*, 14372; [18b] M. Zhang, H. Fan, X. Guo, Y. He, Z. Zhang, J. Min, J. Zhang, G. Zhao, X. Zhan, Y. Li, *Macromolecules* **2010**, *43*, 5706.

[19] K.-C. Li, J.-H. Huang, Y.-C. Hsu, P.-J. Huang, C.-W. Chu, J.-T. Lin, K.-C. Ho, K.-H. Wei, H.-C. Lin, *Macromolecules* **2009**, *42*, 3681.

[20] I. H. Jung, Y. K. Jung, J. Lee, J.-H. Park, H. Y. Woo, J.-I. Lee, H. Y. Chu, H.-K. Shim, *J. Polym. Sci., Part A: Polym. Chem.* **2008**, *46*, 7148.

[21] [21a] L. Huo, C. He, M. Han, E. Zhou, Y. Li, *J. Polym. Sci., Part A: Polym. Chem.* **2007**, *45*, 3861; [21b] G.-Y. Chen, C.-M. Chiang, D. Kekuda, S.-C. Lan, C.-W. Chu, K.-H. Wei, *J. Polym. Sci., Part A: Polym. Chem.* **2010**, *48*, 1669.

[22] N. Kleinhenz, L. Yang, H. Zhou, S. C. Price, W. You, *Macromolecules* **2011**, *44*, 872.